

Electron Transfer in Weakly
Interacting Systems

NORMAN SUTIN AND BRUCE S. BRUNSCHWIG

Department of Chemistry
Brookhaven National Laboratory
Upton, New York 11973

DISCLAIMER

A recently proposed semiclassical model, in which an electronic transmission coefficient and a nuclear tunneling factor are introduced as corrections to the classical activated-complex expression, is described. The nuclear tunneling corrections are shown to be important only at low temperatures or when the electron transfer is very exothermic. By contrast, corrections for nonadiabaticity may be significant for most outer-sphere reactions of metal complexes. The rate constants for the $\text{Fe}(\text{H}_2\text{O})_6^{2+}$ - $\text{Fe}(\text{H}_2\text{O})_6^{3+}$, $\text{Ru}(\text{NH}_3)_6^{2+}$ - $\text{Ru}(\text{NH}_3)_6^{3+}$ and $\text{Ru}(\text{bpy})_3^{2+}$ - $\text{Ru}(\text{bpy})_3^{3+}$ electron exchange reactions predicted by the semiclassical model are in very good agreement with the observed values. The implications of the model for optically-induced electron transfer in mixed-valence systems are noted.

The study of electron transfer reactions in solution is characterized by a strong interplay of theory and experiment.

Theory has suggested systems for study, and experiments have suggested modifications to the theory. Although a number of theories have been proposed (1-14), there is general agreement that the crux of the electron transfer problem is the fact that the equilibrium nuclear configuration of a species changes when it gains or loses an electron. In the case of a metal complex, this configuration change involves changes in the metal-ligand and intraligand bond lengths and angles as well as changes in the vibrations and orientations of the surrounding solvent dipoles. In view of these configuration changes, the rate constants for electron transfer reactions are determined by nuclear as well as electronic factors. The first factor depends on the difference in the nuclear configurations of the reactants and products; the smaller this difference, the more rapid the reaction. The second factor is a function of the electronic interaction of the two reactants; the larger this interaction, the more rapid the electron transfer.

Since the electronic interaction of the two reactants becomes more favorable with decreasing separation, the most favorable configuration for electron transfer is generally one in which the two reactants are in close proximity. Opposing this effect is the coulombic work required to bring similarly-charged reactants together, and ultimately the electron-electron repulsions. Thus in bimolecular reactions the electron transfer may occur over a range of separation distances. Consequently, in

order to obtain the rate constant for the electron transfer, it is necessary to integrate with respect to the separation distance:

$$k = \int_0^{\infty} \frac{4\pi N r^2}{1000} g(r) k_{e1}(r) dr \quad (1)$$

In this equation $g(r)$ is the equilibrium radial distribution function for a pair of reactants, $g(r)4\pi r^2 dr$ is the probability that the centers of the pair of reactants are separated by a distance between r and $r + dr$, and $k_{e1}(r)$ is the (first-order) rate constant for electron transfer at the separation distance r . Intramolecular electron transfer reactions involving "floppy" bridging groups can, of course, also occur over a range of separation distances.

In the conventional Debye-Hückel treatment (15) the radial distribution function for a pair of reactants is simply equal to $\exp(-w/RT)$ with w given by

$$w = \left(\frac{z_2 z_3 e^2}{D_s r} \right) \left[\frac{\exp(\beta \sigma \sqrt{\mu})}{1 + \beta \sigma \sqrt{\mu}} \right] \exp(-\beta r \sqrt{\mu}) \quad (2)$$

where z_2 and z_3 are the charges on the two reactants, D_s is the static dielectric constant of the medium, σ is the distance of closest approach of the centers of the two reactants (that is, the sum of their hard-sphere radii) and β is given by

$$\beta = \left(\frac{8\pi N e^2}{1000 D_s kT} \right)^{1/2} \quad (3)$$

Although more complex pair-correlation functions are available, the Debye-Hückel expression is adequate for our present purpose. It is valid provided that the work required to bring the reactants together is predominantly coulombic, and the ionic strength is low.

Classical Formalism

In the classical formalism it is assumed that bimolecular electron transfer occurs in a precursor complex in which the reactants are separated by the close-contact distance σ (16). Under these conditions the activation-controlled rate constant is given by the product of K_A , the equilibrium constant for the formation of the precursor complex, and $k_{e2}(\sigma)$, the first-order rate constant for electron transfer within the precursor complex:

$$k = K_A k_{e2}(\sigma) \quad (4a)$$

$$K_A = \frac{4\pi N\sigma^3}{3000} \exp\left[-\frac{w(\sigma)}{RT}\right] \quad (4b)$$

$$w(\sigma) = \frac{z_2 z_3 e^2}{D_S \sigma (1 + 8\sigma \sqrt{\mu})} \quad (5)$$

The above expression for K_A has been derived from free volume considerations (17) as well as from the forward and reverse rates of diffusion-controlled reactions (18). The relation between the above formulation and eq 1 may be seen from the following considerations. If most of the contribution to the observed rate comes from electron transfer over a small range of r values then

$$k \sim \frac{4\pi N r^2}{1000} \delta r g(\bar{r}) k_{e2}(\bar{r}) \quad (6)$$

where \bar{r} is the value of r corresponding to the maximum value of the integrand and δr is the range of r values over which the rate is appreciable (19). For typical outer-sphere reactions $r = \sigma \sim 6-8 \text{ \AA}$ and, provided that the reaction does not border on the nonadiabatic, $\delta r \sim 2 \text{ \AA}$. Under these conditions the rate constants calculated from eq 4 and 1 will not differ significantly. (In the original Marcus formulation (1) a collision number Z , equal to $10^{11} \text{ M}^{-1} \text{ s}^{-1}$, replaces $4\pi N_0^3/3000$.)

We next consider the expression for k_{el} in the classical formalism. According to the Franck-Condon principle, internuclear distances and nuclear velocities do not change during the actual electron transfer. This requirement is incorporated into the classical electron-transfer theories by postulating that the electron transfer occurs at the intersection of two potential energy surfaces, one for the reactants (precursor complex) and the other for the products (successor complex). This is illustrated in Figure 1. The Franck-Condon principle is obeyed since the nuclear configurations and energies of the reactants and products are the same at the intersection. It is further assumed that the electron transfer occurs with unit probability in the intersection region, that is, the reaction is assumed to be adiabatic. In terms of the surfaces in Figure 1, H_{AB} , the electronic coupling of the initial and final states, is assumed to be large enough so that the system remains on the

lower potential energy surface on passing through the intersection region, but small enough so that it may be neglected in calculating the height of the potential barrier ($H_{AB} \ll E_{th}$). Under these conditions the rate constant for the conversion of the precursor to the successor complex is independent of the magnitude of the electronic coupling and depends only on the nuclear factor

$$k_{el} = \nu_n \exp(-(\Delta G_{in}^* + \Delta G_{out}^*)/RT) \quad (7)$$

where ν_n is the effective (nuclear) frequency with which the system crosses the barrier and ΔG_{in}^* and ΔG_{out}^* are the contributions of the inner-shell and outer-shell (solvent) reorganizations to the free energy barrier. The effective frequency (8) and the reorganization energies (1,2) for an exchange reaction are given by

$$\nu_n = \left[\frac{\nu_{in} 2\Delta G_{in}^* + \nu_{out} 2\Delta G_{out}^*}{\Delta G_{in}^* + \Delta G_{out}^*} \right]^{1/2} \quad (8)$$

$$\Delta G_{in}^* = \frac{1}{2} \sum f_i (\Delta d_i^0/2)^2 \quad (9)$$

$$\Delta G_{out}^* = \frac{(\Delta e)^2}{4} \left[\frac{1}{2a_2} + \frac{1}{2a_3} - \frac{1}{r} \right] \left[\frac{1}{D_{op}} - \frac{1}{D_s} \right] \quad (10)$$

In the above expressions ν_{in} is the average metal-ligand stretching frequency ($300-500 \text{ cm}^{-1}$), ν_{out} is an average solvent orientation frequency (the vibrational spectrum of water exhibits a number of bands with a major band at $\sim 1 \text{ cm}^{-1}$ and with additional bands at higher frequency; 30 cm^{-1} is used here as an

average frequency), f_i is a reduced force constant equal to $2f_i^A f_i^B / (f_i^A + f_i^B)$ where f_i^A and f_i^B are the force constants for the i th vibration in the one reactant in its initial and final states (i.e. in its oxidized and reduced forms, and vice versa for the other reactant), $\Delta d_i^O = |d_i^A - d_i^B|$ where d_i^A and d_i^B are the corresponding equilibrium bond distances (the sum is over all the vibrations of the reactants), a_2 and a_3 are the radii of the two reactants, $r = \sigma = (a_2 + a_3)$, and D_{Op} is the optical dielectric constant of the medium (equal to the square of the refractive index).

The inner-shell and outer-shell distortions of the reactants leading to the activated complex are illustrated in Figure 2. The ellipses depict equipotential sections through the potential energy surfaces for the precursor and successor complexes. The initial distortion of the precursor complex is predominantly along the low-frequency solvent coordinate. When the solvent configuration appropriate to the activated complex has been reached, the system continues to ascend to the top of the barrier by distorting primarily along the inner-sphere coordinate (defined by the steepest descent pathway). The electron transfer occurs at the top of the barrier and the system passes over the barrier with an effective frequency ν_n to form the successor complex.

Comparison of Observed and Calculated Exchange Rate

Constants. The rate constants for the $\text{Fe}(\text{H}_2\text{O})_6^{2+} - \text{Fe}(\text{H}_2\text{O})_6^{3+}$, $\text{Ru}(\text{NH}_3)_6^{2+} - \text{Ru}(\text{NH}_3)_6^{3+}$ and $\text{Ru}(\text{bpy})_3^{2+} - \text{Ru}(\text{bpy})_3^{3+}$ exchange reactions calculated from eq 4,5 and 7-10 are compared with the

observed values in Table I. The agreement of the calculated and observed rate constants for the $\text{Fe}(\text{H}_2\text{O})_6^{2+} - \text{Fe}(\text{H}_2\text{O})_6^{3+}$ exchange is very good for $\Delta d^0 = 0.14 \text{ \AA}$ while the agreement of the calculated and observed rate constants is less satisfactory for the $\text{Ru}(\text{NH}_3)_6^{2+} - \text{Ru}(\text{NH}_3)_6^{3+}$, for the $\text{Ru}(\text{bpy})_3^{2+} - \text{Ru}(\text{bpy})_3^{3+}$ and for the $\text{Fe}(\text{H}_2\text{O})_6^{2+} - \text{Fe}(\text{H}_2\text{O})_6^{3+}$ exchange for $\Delta d^0 = 0.11 \text{ \AA}$. The slow rate of the $\text{Fe}(\text{H}_2\text{O})_6^{2+} - \text{Fe}(\text{H}_2\text{O})_6^{3+}$ exchange is a consequence of large inner-shell and solvent reorganization barriers. By contrast, the $\text{Ru}(\text{bpy})_3^{2+} - \text{Ru}(\text{bpy})_3^{3+}$ exchange is very rapid because of its negligible inner-shell and small solvent reorganization barrier. The $\text{Ru}(\text{NH}_3)_6^{2+} - \text{Ru}(\text{NH}_3)_6^{3+}$ exchange is intermediate in character, but with the bulk of the barrier arising from ΔG_{out}^* .

Semiclassical Formalism

In the classical activated-complex formalism nuclear tunneling effects are neglected. In addition, the electron transfer is assumed to be adiabatic. These assumptions are relaxed in the semiclassical model.

The electron transfer process is characterized by the frequencies shown in Table II.

Table II. Characteristic frequencies for electron transfer

electronic (delocalized orbital)	$10^{15} - 10^{16} \text{ s}^{-1}$
vibrational (M-L, C-H, O-H)	$10^{13} - 10^{14} \text{ s}^{-1}$ $300 - 3000 \text{ cm}^{-1}$
orientational (solvent dipoles)	$10^{11} - 10^{12} \text{ s}^{-1}$ $3 - 30 \text{ cm}^{-1}$

The difference in the time scales for electronic and nuclear motions is, of course, the basis of the Born-Oppenheimer approximation (and the Franck-Condon principle). This approximation allows for the separation of nuclear and electronic coordinates in the wave equation and is implicit in the calculation of the potential energy surfaces illustrated in Figures 1 and 2. Such surfaces describe the electronic energy of the system as a function of the nuclear coordinates.

Classically, the rate of electron transfer is determined by the rate of passage of the system over the barrier defined by the surfaces. In the semiclassical model (13) a nuclear tunneling factor that measures the increase in rate arising from quantum-mechanical tunneling through the barrier is included. In addition, the possibility that the electron transfer may not occur even when the nuclear configurations of the reactants are appropriate (for example, when the reactants are far apart or the electron transfer is spin forbidden) is allowed for by introducing an electronic transmission coefficient (13). The rate constant for electron transfer within the semiclassical formalism is thus given by

$$k = \int_{\sigma}^{\infty} \frac{4\pi N r^2}{1000} \exp\left[-\frac{w(r)}{RT}\right] \kappa(r) \Gamma_n \nu_n(r) \exp\left[-\frac{(\Delta G_{in}^* + \Delta G_{out}^*(r))}{RT}\right] dr \quad (11)$$

where κ is the electronic transmission factor and Γ_n is the nuclear tunneling factor. These factors are considered in turn.

Nuclear tunneling. Nuclear tunneling is important for a particular mode when $h\nu > kT$. Since $\nu_{in} > \nu_{out}$ nuclear tunneling will be more important for the inner-sphere than for the solvent modes. For the purposes of the present discussion we will assume that nuclear tunneling of the solvent modes may be neglected, that is, we assume that it is necessary for the solvent to acquire the nuclear configuration appropriate to the top of the barrier (activated complex) as a prerequisite for electron transfer. This assumption is probably valid above 50 K. Because of nuclear tunneling it is not necessary for the inner-sphere to achieve the configuration of the activated complex; rather electron transfer may occur at any inner-sphere configuration. This is illustrated in Figure 3.

According to a recent model (13) nuclear tunneling factors for the inner-sphere modes can be defined by

$$\ln \Gamma_n = (\Delta G_{in}^* - \Delta G_{in}(T))/RT$$

where $\Delta G_{in}(T)$ is a temperature-dependent inner-shell reorganization energy that approaches the classical value ΔG_{in}^* at high temperature. A particularly useful expression for $\Delta G_{in}(T)$ is obtained using Holstein's saddle-point method (13,29). Use of this expression leads to the following expression for the first-order rate constant for an exchange reaction

$$k_{el} = \kappa \nu_n \exp \left\{ -\frac{E_{in}}{Nh\nu_{in}} \tanh \left[\frac{Nh\nu_{in}}{4RT} \right] - \frac{E_{out}}{4RT} \right\} \quad (12)$$

where $E_{in} \sim 4\Delta G_{in}^*$ and $E_{out} \sim 4\Delta G_{out}^*$. An equivalent approach (13) leads to the following expression for Γ_n

$$\Gamma_n = A \sum_m \exp \left\{ -\frac{\epsilon_m}{RT} \right\} S_{m,m}^2 \quad (13)$$

where A is a normalization factor, $S_{m,m}^2$ is the square of the overlap (Franck-Condon factor) of the m^{th} vibrational state of the reactants with the m^{th} vibrational state of the products, and ϵ_m is the energy of the m^{th} vibrational level. (See Figure 4; note that this formalism is very similar to one proposed in an early paper (30) on the basis of a perceived analogy between electron transfer reactions and ordinary electronic transitions.)

The value of $\log \Gamma_n$ for the $\text{Fe}(\text{H}_2\text{O})_6^{2+} - \text{Fe}(\text{H}_2\text{O})_6^{3+}$ exchange (which features a relatively large inner-sphere barrier) is plotted as a function of $1/T$ in Figure 5. The nuclear tunneling factors are close to unity at room temperature but become very large at low temperatures. As a consequence of nuclear tunneling, the electron transfer rates at low temperatures will be much faster than those calculated from the classical model.

The value of $\log \Gamma_n$ at 300 K for a (hypothetical) $\text{Fe}(\text{H}_2\text{O})_6^{2+} - \text{Fe}(\text{H}_2\text{O})_6^{3+}$ exchange reaction is plotted as a function of ΔG° in Figure 6. The nuclear tunneling factors at first decrease and then become very large at high driving force. The dramatic increase in Γ_n corresponds to the onset of the inverted free-energy region of the classical formalism (1). Although nuclear tunneling will reduce the magnitude of the rate decreases predicted for the inverted region, substantial rate decreases are still expected. There is only meager experimental support for the predicted rate decreases and this area is currently receiving much attention (31-35).

The Effective Nuclear Frequency. When nuclear tunneling is important we suggest that the individual frequencies should be

weighted by their effective barriers, that is, instead of eq 8 it may be more appropriate to use eq 14

$$\nu_n = \left(\frac{\frac{h\nu_{in}^3}{2kT} E_{in} \operatorname{csch} 2\nu_{in}' + \nu_{out}^2 E_{out}}{\frac{h\nu_{in}}{2kT} E_{in} \operatorname{csch} 2\nu_{in}' + E_{out}} \right)^{1/2} \quad (14)$$

in which E_{in} has been replaced by its quantum-mechanical analogue $2\nu_{in}' E_{in} \operatorname{csch} 2\nu_{in}'$ where $\nu_{in}' = Nh\nu_{in}/4RT = h\nu_{in}/4kT$. It should be noted that the effective nuclear frequency tends towards the solvent frequency when nuclear tunneling by the inner-sphere modes becomes very important. However, in most cases at room temperature ν_n approaches ν_{in} .

Electronic Transmission Coefficient. The probability that the electron transfer will occur in the intersection region (in other words, the probability that the system will remain on the lower adiabatic surface on passing through the intersection region) is given by

$$\kappa = \frac{2(1 - \exp(-\nu_{e2}/2\nu_n))}{2 - \exp(-\nu_{e2}/2\nu_n)} \quad (15)$$

where ν_{e2} , the frequency of electron transfer within the activated complex, is given by

$$\nu_{e2} = \frac{2H_{AB}^2}{h} \left(\frac{\pi^3}{(E_{in} + E_{out})RT} \right)^{1/2} \quad (16)$$

(The ν_{e2} defined here should not be confused with the electronic frequency ν_{e2}^0 in Table II which is the frequency for

a fully delocalized electron. When the interaction between the potential energy surfaces is very large then $\nu_{el} \rightarrow \nu_{el}^0$. Also, when nuclear tunneling is important E_{in} in the denominator should be replaced by $2\nu_{in}'E_{in}$ csch $2\nu_{in}'$.) It is evident from eq 15 that $\kappa = 1$ (the electron transfer is adiabatic) when $\nu_{el} \gg 2\nu_n$ and that $\kappa = \nu_{el}/\nu_n$ (the electron transfer is nonadiabatic) when $\nu_{el} \ll 2\nu_n$. In the nonadiabatic limit the frequency factor is an electronic (ν_{el}) rather than a nuclear (ν_n) frequency, that is, the rate constant for a nonadiabatic reaction is

$$k = \int_{\sigma}^{\infty} \frac{4\pi N r^2}{1000} \exp\left[-\frac{w(r)}{RT}\right] \nu_{el}(r) \Gamma_n \exp\left[-\frac{(\Delta G_{in}^* + \Delta G_{out}^*(r))}{RT}\right] dr \quad (17)$$

The reason for the absence of the nuclear frequency from eq 17 is that the slowest process in a nonadiabatic reaction is, by definition, the electron transfer; that is, $\nu_{el} \ll \nu_n$ for a nonadiabatic reaction.

The magnitude of the electronic interaction between the reactants is very important. If H_{AB} is very small then the coupling of the initial and final states of the system will be very weak, the electron transfer will be slow, and the reaction will be nonadiabatic. The procedures used for estimating H_{AB} or κ include the following:

- (a) Ab initio calculations (4,37).
- (b) Approximate theoretical models (38,39).
- (c) Intensities of charge-transfer bands: H_{AB} may be estimated from the intensity of the intervalence charge-transfer

band in mixed-valence systems using the Hush relation (36)

$$H_{AB} = \frac{2.06}{r} \left(\epsilon_{\max} \bar{\nu}_{\max} \Delta \bar{\nu}_{1/2} \right)^{1/2} \text{ cm}^{-1} \quad (18)$$

where ϵ_{\max} is the molar absorptivity at the absorbance maximum $\bar{\nu}_{\max}$, and $\Delta \bar{\nu}_{1/2}$ is the full width of the band at half maximum.

(d) Temperature dependence of the rate: κ can be estimated from the entropy of activation for the electron-transfer reaction. However this procedure must be used with caution since nuclear tunneling contributions and the temperature dependence of the electrostatic work terms will also tend to make the entropy of activation more negative.

(e) The limiting rate constant at high driving force: normally $k \rightarrow k_d$, the diffusion-controlled rate constant, as ΔG° increases. However if κ is small then $k \rightarrow K_A \kappa \nu_{\text{eff}}$ as ΔG° increases ($\Delta G^* \rightarrow 0$). Thus κ can be obtained if rate saturation below the diffusion limit is observed. (Care must be exercised in this case, too, since rate saturation below the diffusion limit may be observed for other reasons, including a preequilibrium change on one of the reactants (40,41), substitution control (42), etc.)

Values of H_{AB} and κ obtained using the first three procedures are presented in Table III. On the basis of Newton's calculations, the $\text{Fe}(\text{H}_2\text{O})_6^{2+} - \text{Fe}(\text{H}_2\text{O})_6^{3+}$ exchange at $r = 6.4 \text{ \AA}$ is nonadiabatic. On the other hand, calculations for the $\text{Cr}(\text{H}_2\text{O})_6^{2+} - \text{Cr}(\text{H}_2\text{O})_6^{3+}$ exchange performed by Hush indicate that this exchange is adiabatic. In contrast to the $\text{Fe}(\text{H}_2\text{O})_6^{2+} - \text{Fe}(\text{H}_2\text{O})_6^{3+}$ exchange, in which the two oxidation

states differ by an electron in a t_{2g} orbital, in the $\text{Cr}(\text{H}_2\text{O})_6^{2+} - \text{Cr}(\text{H}_2\text{O})_6^{3+}$ exchange the two oxidation states differ by an e_g electron. Evidently the electronic coupling in the latter exchange, but not the former, is considerably enhanced by mixing in the orbitals of the intervening water molecules. Based on direct $4d - 4d$ overlap, the $\text{Ru}(\text{NH}_3)_6^{2+} - \text{Ru}(\text{NH}_3)_6^{3+}$ exchange is barely adiabatic while the $\text{Ru}(\text{bpy})_3^{2+} - \text{Ru}(\text{bpy})_3^{3+}$ exchange is highly nonadiabatic! Presumably the delocalization of the metal t_{2g} electron density onto the π^* orbitals of the bipyridine ligands is what makes the $\text{Ru}(\text{bpy})_3^{2+} - \text{Ru}(\text{bpy})_3^{3+}$ exchange so rapid. Estimates of the magnitude of the electronic coupling provided by the $\pi^* - \pi^*$ interaction of the two reactants are consistent with this interpretation (42).

Table III also includes values of H_{AB} and κ estimated from the properties of the intervalence band observed for mixed-valence diruthenium complexes. Coupling by the pyrazine in these complexes is very strong and is particularly striking when compared with the coupling provided by the through-space interaction of two ruthenium centers at comparable r as manifested in the $\text{Ru}(\text{NH}_3)_6^{2+} - \text{Ru}(\text{NH}_3)_6^{3+}$ exchange. Coupling of the ruthenium centers by the 4,4'-bipyridine group is strong enough for the intramolecular electron exchange to be adiabatic. Introduction of a $-\text{CH}_2-$ group between the two pyridine rings reduces the coupling so that the electron transfer becomes nonadiabatic.

For many purposes H_{AB} may be approximated by (38,39)

$$H_{AB} = H_{AB}^0 \exp(-\beta'(r-\sigma)) \quad (19)$$

where H_{AB}^0 is the value of H_{AB} at $r = \sigma$. The values of β' are 1.7 \AA^{-1} for the $\text{Fe}(\text{H}_2\text{O})_6^{2+} - \text{Fe}(\text{H}_2\text{O})_6^{3+}$ exchange at $r \sim \sigma$ (35), 2.5 \AA^{-1} for the $\text{Cr}(\text{H}_2\text{O})_6^{2+} - \text{Cr}(\text{H}_2\text{O})_6^{3+}$ exchange at $r \sim \sigma$ (4), and $\sim 1.0 \text{ \AA}^{-1}$ for two parallel aromatic rings such as anthracene and its radical anion (39).

An important conclusion that can be drawn from the above discussion is that most outer-sphere electron transfer reactions of metal complexes are, at best, marginally adiabatic and that the reaction will rapidly become nonadiabatic with increasing separation of the reactants. In view of these considerations, eq 11 can be integrated to give the following expression:

$$k = \frac{4\pi N \sigma^2}{2000\beta'} \exp\left[-\frac{w(\sigma)}{RT}\right] \kappa(\sigma) \Gamma_n \nu_n(\sigma) \exp\left[-\frac{(\Delta G_{in}^* + \Delta G_{out}^*(\sigma))}{RT}\right] \quad (20)$$

Inspection of eq 20 shows that the effective δr for a nonadiabatic reaction is $1/2\beta'$. Thus for $\beta' = 1.7 \text{ \AA}^{-1}$, δr for a nonadiabatic reaction is $\sim 1/5$ that for an adiabatic reaction at comparable σ .

We next reconsider the systems in Table I in the light of eq 20. The results of the calculations are presented in Table IV which includes the classical and experimental results. The rate constants for the $\text{Ru}(\text{NH}_3)_6^{2+} - \text{Ru}(\text{NH}_3)_6^{3+}$ and $\text{Ru}(\text{bpy})_3^{2+} - \text{Ru}(\text{bpy})_3^{3+}$ exchanges calculated from the semiclassical expressions are in much better agreement with the observed values

than are the rate constants given by the classical expressions. The semiclassical calculation also gives good agreement with the observed rate constant for the $\text{Fe}(\text{H}_2\text{O})_6^{2+} - \text{Fe}(\text{H}_2\text{O})_6^{3+}$ exchange if the EXAFS value of Δd^0 (0.11 Å) rather than the crystallographic value (0.14 Å) is used. (Use of the smaller Δd^0 value lowers the inner-shell reorganization barrier leaving more room for nonadiabaticity; use of the crystallographic value of Δd^0 leads to a calculated rate constant that is much lower than the observed value if $\kappa \sim 10^{-2}$.) Note that the calculated rate constants for the $\text{Ru}(\text{NH}_3)_6^{2+} - \text{Ru}(\text{NH}_3)_6^{3+}$ and $\text{Ru}(\text{bpy})_3^{2+} - \text{Ru}(\text{bpy})_3^{3+}$ exchanges are, if anything, larger than the observed values.

Conclusions

The above discussion shows that very good agreement of observed and calculated exchange rate constants can be obtained using the semiclassical formalism. This formalism allows for the different characteristic time scales (Table II) in a natural manner. The fastest motion, that of the electrons (ν_{el}^0), defines the potential energy surfaces for the reaction. The slower nuclear processes (in this discussion, the solvent motion) take place on the surface and define a classical barrier for the reaction ΔG_{out}^* . By contrast, the faster nuclear processes (here, the inner-sphere motion) are not required to remain on the surface; rather they can tunnel through the barrier $\Delta G_{in}(T)$. Finally, the slower of the electron hopping (ν_{el}) and the average nuclear (ν_n) frequencies becomes a prefactor in the rate expression.

Nonequilibrium effects. In applying the various formalisms, a Boltzmann distribution over the vibrational energy levels of the initial state is assumed. If the electron transfer is very rapid ($\nu_{el} \gg \nu_{in} > \nu_{out}$) then the equilibrium distribution over the energy levels may not be maintained. (One consequence of this is the breakdown of the Born-Oppenheimer approximation when the electronic coupling becomes very strong.)

A nonequilibrium distribution of nuclear configurations can, of course, be deliberately produced by optical excitation of the system. In this case the state immediately formed possesses the inner-sphere and the solvent configuration of the initial state but the electronic configuration of the final state (Figure 1). Relaxation to the nuclear configuration appropriate to the final state requires both inner-sphere and solvent reorganization. The former will occur rapidly, the latter only relatively slowly. Consequently the initially formed state will first relax to an intermediate state having the inner-sphere configuration appropriate to the final electronic configuration, but with a solvent configuration which is still appropriate to the initial electronic configuration. At this stage solvent relaxation to the final state competes with back electron-transfer to the initial state. The quantum yield for the formation of the final state will be approximately equal to $\nu_{out}/(\kappa\nu_{in} + \nu_{out})$ which is $\ll 1$ when $\kappa \sim 1$. This type of explanation can account for the

low yields ($< 10\%$) of the electronic isomer formed after optical excitation in the intervalence band of certain mixed-valence systems (50). Although formation of the final state will be favored if the electronic coupling is very weak ($\kappa \ll 1$), the intensity of the intervalence transition will also be very weak under these conditions.

To summarize, in this article we have discussed some aspects of a semiclassical electron-transfer model (13) in which quantum-mechanical effects associated with the inner-sphere are allowed for through a nuclear tunneling factor, and electronic factors are incorporated through an electronic transmission coefficient or adiabaticity factor. We focussed on the various time scales that characterize the electron transfer process and we presented one example to indicate how considerations of the time scales can be used in understanding nonequilibrium phenomena.

Acknowledgments. The authors wish to acknowledge very helpful discussions with Dr. C. Creutz. This research was supported by the Office of Basic Energy Sciences of the U. S. Department of Energy.

Literature Cited

1. Marcus, R. A. Annu. Rev. Phys. Chem. 1964, 15, 155.
2. Marcus, R. A. J. Chem. Phys. 1965, 43, 679.
3. Hush, N. S. Trans. Faraday Soc. 1961, 57, 557.
4. Hush, N. S. Electrochim. Acta 1968, 13, 1005.
5. Kestner, R. N.; Logan, J.; Jortner, J. J. Phys. Chem. 1974, 78, 2148.
6. Dogonadze, R. R.; Kuznetsov, A. M.; Levich, V. G. Electrochim. Acta 1968, 13, 1025.
7. German, E. D.; Dvali, V. G., Dogonadze, R. R.; Kuznetsov, A. M. Elektrckimiya 1976, 12, 639.
8. Dogonadze, R. R. In "Reactions of Molecules at Electrodes", Hush, N. S., Ed.; Wiley-Interscience: New York, 1971; Chapter 3, p 135.
9. Van Duyne, R. P.; Fischer, S. F. Chem. Phys. 1974, 5, 183.
10. Ulstrup, J.; Jortner, J. J. Chem. Phys. 1975, 63, 4358.
11. Efrima, S.; Bixon, M. Chem. Phys. 1976, 13, 447.
12. Chance, B., DeVault, D. C., Frauenfelder, H., Marcus, R. A., Schrieffer, J. B., Sutin, N. Eds. "Tunneling in Biological Systems"; Academic Press: New York, 1979.
13. Brunshwig, B. S.; Logan, J.; Newton, M. D.; Sutin, N. J. Am. Chem. Soc. 1980, 102, 5798.
14. Ulstrup, J. "Charge Transfer Processes in Condensed Media"; Springer-Verlag: West Berlin, 1979.

15. Pitzer, K. S. Acc. Chem. Res. 1977, 10, 371.
16. Brown, G. M.; Sutin, N. J. Am. Chem. Soc. 1979, 101, 883.
17. Fuoss, R. M. J. Am. Chem. Soc. 1958, 30, 5059.
18. Eigen, M. Z. Phys. Chem. (Frankfurt am Main) 1954, 1, 176.
19. Reynolds, W. L.; Lumry, R. W. "Mechanisms of Electron Transfer"; Ronald Press: New York, 1966.
20. Hair, N. J.; Beattie, J. K. Inorg. Chem. 1977, 16, 245.
21. Sham, T. K.; Hastings, J. M.; Perlman, M. L. J. Am. Chem. Soc. 1980, 102, 5904.
22. Stynes, H. C.; Ibers, J. A. Inorg. Chem. 1971, 10, 2304.
23. Zalkin, A.; Templeton, D. H.; Ueki, T. Inorg. Chem. 1973, 12, 1641.
24. Baker, J.; Engehardt, L. M.; Figgis, B. N.; White, A. H. J. Chem. Soc., Dalton Trans. 1975, 530.
25. Silverman, J.; Dodson, R. W. J. Phys. Chem. 1952, 56, 846.
26. Meyer, T. J.; Taube, H. Inorg. Chem. 1968, 7, 2369.
27. Biradar, N.S.; Stranks, D. R. Trans. Faraday Soc. 1963, 58, 2421.
28. Young, R. C.; Keene, F. R.; Meyer, T. J. J. Am. Chem. Soc. 1977, 99, 2468.
29. Holstein, T. Philos. Mag. 1978, 37, 49.
30. Sutin, N. Annu. Rev. Nucl. Sci. 1962, 12, 285.
31. Creutz, C.; Sutin, N. J. Am. Chem. Soc. 1977, 99, 241.
32. Ballardini, R.; Varani, G.; Indelli, M. T.; Scandola, F.; Balzani, V. J. Am. Chem. Soc. 1978, 100, 7219.
33. Nagle, J. K.; Dressick, W. J.; Meyer, T. J. J. Am. Chem. Soc. 1979, 101, 3993.

34. Bock, C. R.; Connor, J. A.; Gutierrez, A. R.; Meyer, T. J.; Whitten, D. G.; Sullivan, B. P.; Nagle, J. K. J. Am. Chem. Soc. 1979, 101, 4815.
35. Beitz, J. V.; Miller, J. R. J. Chem. Phys. 1979, 71, 4579.
36. Hush, N. S. Prog. Inorg. Chem. 1967, 8, 391.
37. Newton, M. D. Int. J. Quant. Chem., Symp. 1980, 14, 363.
38. Hopfield, J. J. Proc. Natl. Acad. Sci. U.S.A. 1974, 71, 3640.
39. Buhks, E.; Jortner, J. FEBS Lett. 1980, 109, 117.
40. Marcus, R. A.; Sutin, N. Inorg. Chem. 1975, 14, 213.
41. Hoselton, M. A.; Drago, R. S.; Wilson, L. J.; Sutin, N. J. Am. Chem. Soc. 1976, 98, 6967.
42. Creutz, C.; Sutin, N. In "Inorganic Reactions and Methods", Zuckerman, J. J., Ed.; Springer-Verlag: West Berlin, in press.
43. Sutin, N. In "Inorganic Reactions and Methods", Zuckerman, J. J. Ed.; Springer-Verlag: West Berlin, in press.
44. Newton, M. D. this volume.
45. Rieder, K.; Taube, H.; J. Am. Chem. Soc. 1977, 99, 7891.
46. Tom, G. M.; Creutz, C.; Taube, H. J. Am. Chem. Soc. 1974, 96, 7827.
47. Creutz, C.; Inorg. Chem. 1978, 17, 3723.
48. Creutz, C.; Taube, H. J. Am. Chem. Soc. 1973, 94, 1086.
49. Piepho, S. B.; Krausz, E. R.; Schatz, P. N. J. Am. Chem. Soc. 1978, 100, 2996.
50. Creutz, C.; Kroger, P.; Matsubara, T.; Netzel, T. L.; Sutin, N. J. Am. Chem. Soc. 1979, 101, 5442.

Table I. Comparison of Observed and Calculated Rate
 Constants for Exchange Reactions at 25 °C.

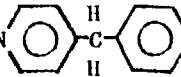
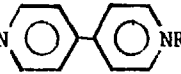
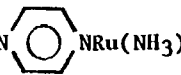
	$\text{Fe}(\text{H}_2\text{O})_6^{2+/3+}$	$\text{Ru}(\text{NH}_3)_6^{2+/3+}$	$\text{Ru}(\text{bpy})_3^{2+/3+}$	Reference
Δd^0 , Å	0.14 ^a , 0.11 ^b	0.04	~ 0	20-24
$(a_2 + a_3)$, Å	6.5	6.7	~ 14	20-24
ΔG_{in}^* , kcal mol ⁻¹	8.34, 5.14	0.76	~ 0	
ΔG_{out}^* , kcal mol ⁻¹	6.92	6.72	3.21	
μ , M	0.55	0.10	0.10	
k_{calcd} , M ⁻¹ s ⁻¹	0.96, 2.2×10^2	2.8×10^5	8.0×10^9 ^c	
k_{obsd} , M ⁻¹ s ⁻¹	4.2	4.3×10^3	4.2×10^8	25-28

^a Crystallographic value of Δd^0 (20).

^b EXAFS value of Δd^0 (21).

^c Not corrected for diffusion.

Table III. Estimates of Electronic Coupling Matrix Elements and Adiabaticity Factors^a

	r	$-H_{AB}$	κ	Reference
	Å	cm ⁻¹		
$\text{Fe}(\text{H}_2\text{O})_6^{2+} \text{Fe}(\text{H}_2\text{O})_6^{3+}$	6.4	31	$\sim 10^{-2}$	<u>37</u>
$\text{Cr}(\text{H}_2\text{O})_6^{2+} \text{Cr}(\text{H}_2\text{O})_6^{3+}$	~ 6.5	~ 180	~ 1	<u>4</u>
$\text{Ru}(\text{NH}_3)_6^{2+} \text{Ru}(\text{NH}_3)_6^{3+}$	6.4	67 ^b	0.2 ^b	<u>37,43</u>
$\text{Ru}(\text{bpy})_3^{2+} \text{Ru}(\text{bpy})_3^{3+}$	14	$\sim 0^c$ $\sim 20-100^d$	$< 10^{-6}^c$ $\sim 1^d$	<u>43</u> <u>43</u>
$[(\text{NH}_3)_5\text{RuN} \text{---} \text{C} \text{---} \text{NRu}(\text{NH}_3)_5]^{5+}$ 	12.3	87	0.2	<u>43,45</u>
$[(\text{NH}_3)_5\text{RuN} \text{---} \text{C} \text{---} \text{NRu}(\text{NH}_3)_5]^{5+}$ 	10.8	400	1.0	<u>43,46,47</u>
$[(\text{NH}_3)_5\text{RuN} \text{---} \text{C} \text{---} \text{NRu}(\text{NH}_3)_5]^{5+}$ 	6.9	~ 3000	---	<u>43,48,49</u>

^a Further details of some of the calculations are given in (43).

^b Most of the electronic interaction is through the H atoms of the ligands (44).

^c Estimated assuming electron transfer by direct 4d-4d overlap.

^d Estimated assuming electron transfer through the π^* orbitals of the bipyridine ring system.

Table IV. Comparison of Semiclassical and Classical Calculations of
Rate Constants for Exchange Reactions at 25 °C^a

	Fe(H ₂ O) ₆ ^{2+/3+}	Ru(NH ₃) ₆ ^{2+/3+}	Ru(bpy) ₃ ^{2+/3+}
$k_{sc}^a, M^{-1} s^{-1}$	$1.3 \times 10^{-3c}, 0.30^d$	7.4×10^3	8.6×10^8
$k_{cl}^b, M^{-1} s^{-1}$	$0.96^c, 2.2 \times 10^{2d}$	2.8×10^5	8.0×10^9
$k_{obsd}, M^{-1} s^{-1}$	4.2	4.3×10^3	4.2×10^8

^a Classical calculation using eq 4,5 and 7-10.

^b Semiclassical calculation using eq 20 together with eq 5, 9,10 and 13-16.

^c Based on crystallographic value of $\Delta d^0 = 0.14 \text{ \AA}$.

^d Based on EXAFS value of $\Delta d^0 = 0.11 \text{ \AA}$.

Figure Captions

Figure 1. Plot of the potential energy of the reactants (precursor complex) and products (successor complex) as a function of nuclear configuration: E_{th} is the barrier for the thermal electron transfer, E_{op} is the energy for the light-induced electron transfer, and the splitting at the intersection of the surfaces is equal to $2H_{AB}$ where H_{AB} is the electronic coupling matrix element. Note that $H_{AB} \ll E_{th}$ in the classical model. The circles indicate the relative nuclear configurations of the two reactants in the precursor complex, optically excited precursor complex, activated complex and successor complex.

Figure 2. Equipotential sections through the potential energy surface for an exchange reaction. The sections define ellipses if the surfaces are parabolic: the top left-hand set refer to the initial state (precursor complex) and the bottom right-hand set refer to the final state (successor complex). The dashed line indicates the reaction coordinate. P_2 and P_3 are parameters reflecting the state of polarization of the solvent and d_2 and d_3 are coordinates reflecting the inner-shell configurations of the two reactants (products).

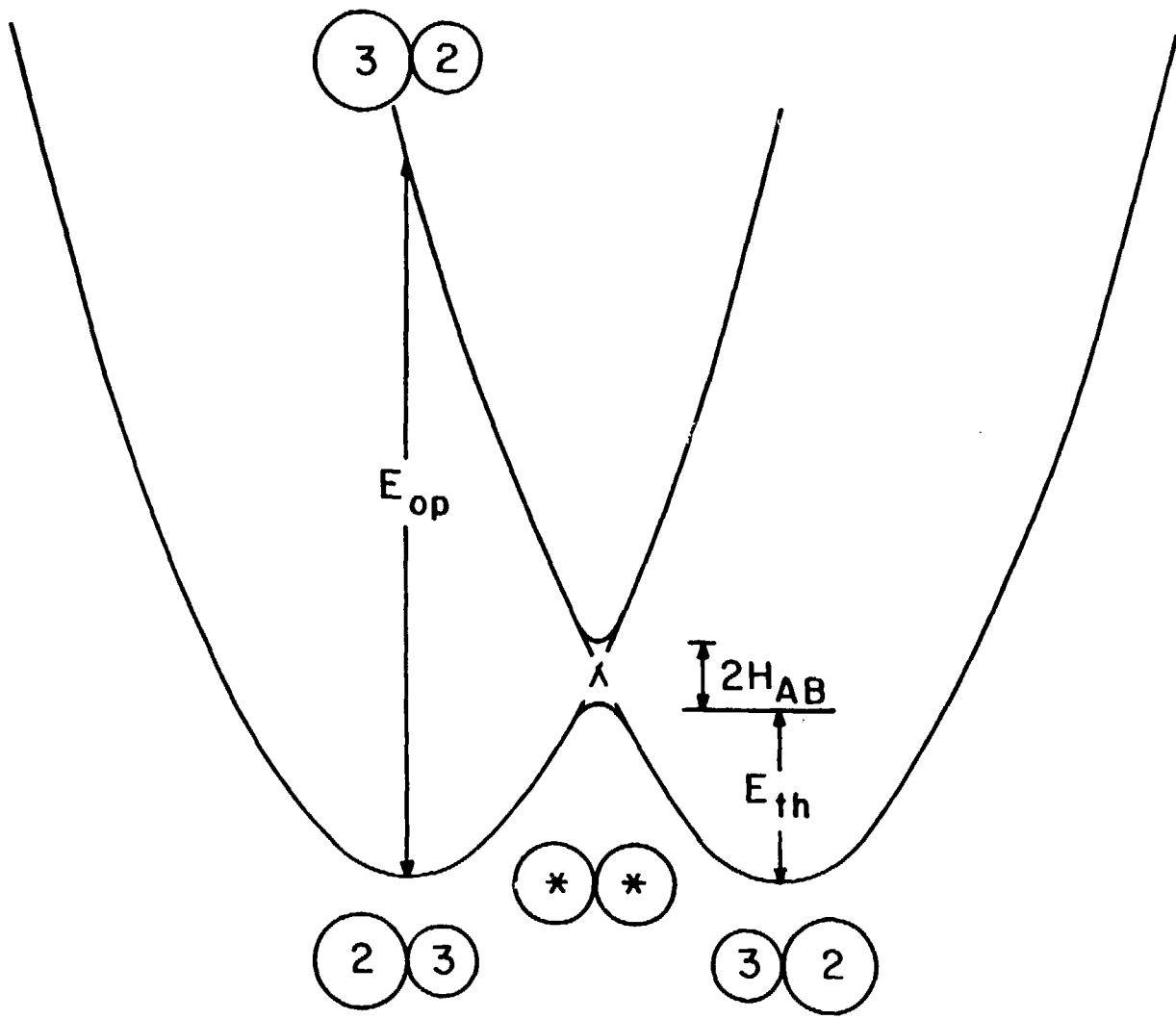
Figure 3. Equipotential sections through the potential energy surface for an exchange reaction, as in Figure 2. The heavy horizontal line indicates the solvent configuration appropriate to the activated complex and is the solvent configuration at which inner-sphere tunneling takes place.

Figure 4. Illustration of inner-sphere tunneling in an exchange reaction. It is assumed that the reactants and products have the same reduced force constant and only the energy levels and wave functions for the lowest vibrational states of the reactants and products are shown.

Figure 5. Plot of the logarithm of the nuclear tunneling factor vs. $1/T$ for the $\text{Fe}(\text{H}_2\text{O})_6^{2+} - \text{Fe}(\text{H}_2\text{O})_6^{3+}$ exchange reaction. The slope of the linear portion below 150 K is equal to $E_{in}/4R$ (13).

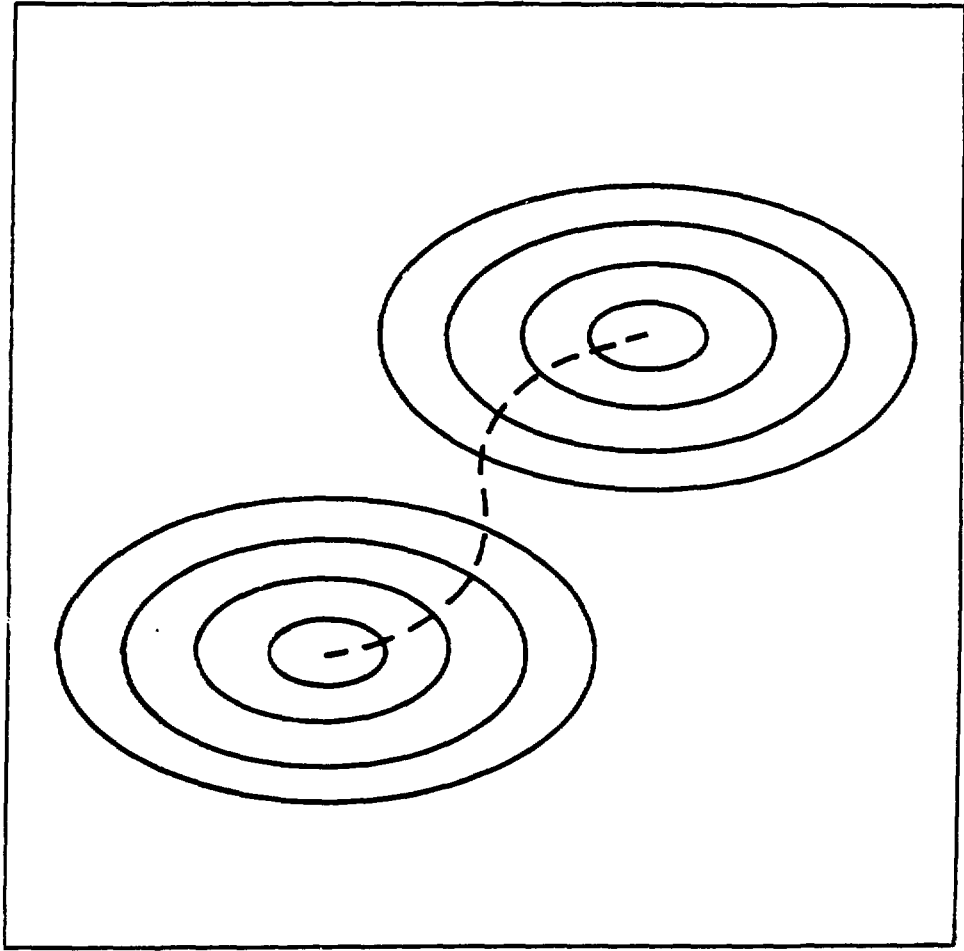
Figure 6. Plot of the logarithm of the nuclear tunneling factor vs. ΔG° for an electron transfer reaction accompanied by a net chemical change: the following parameters were used to calculate $\log \Gamma_n$: $\nu_{in} = 432 \text{ cm}^{-1}$, $\Delta G_{in}^* = 8.34 \text{ kcal mol}^{-1}$, $\Delta G_{out}^* = 0$, $T = 300 \text{ K}$.

POTENTIAL ENERGY



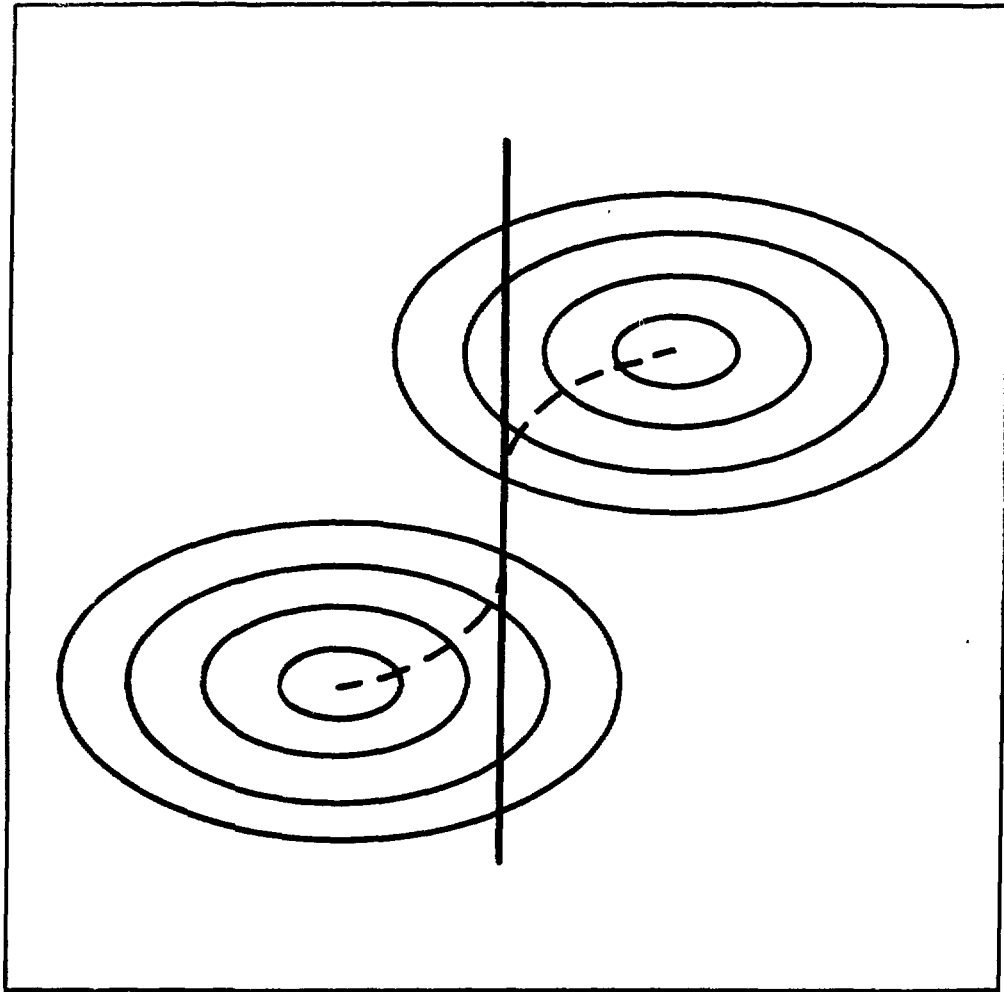
NUCLEAR CONFIGURATION

Figure 1



$(P_2 - P_3)$, solvent

$(d_2 - d_3)$, inner



$(P_2 - P_3)$, solvent

$(d_2 - d_3)$, inner

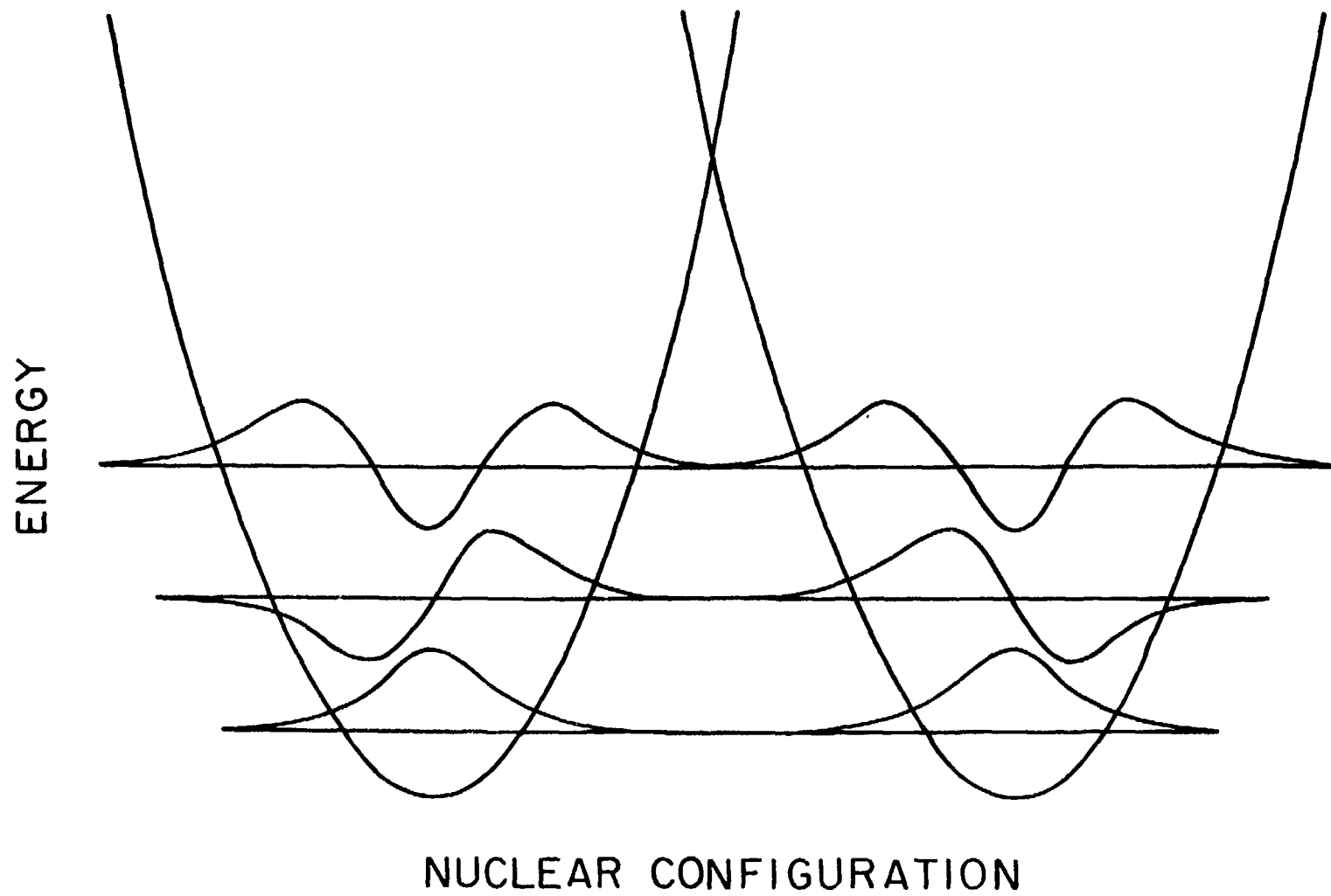


Figure 4

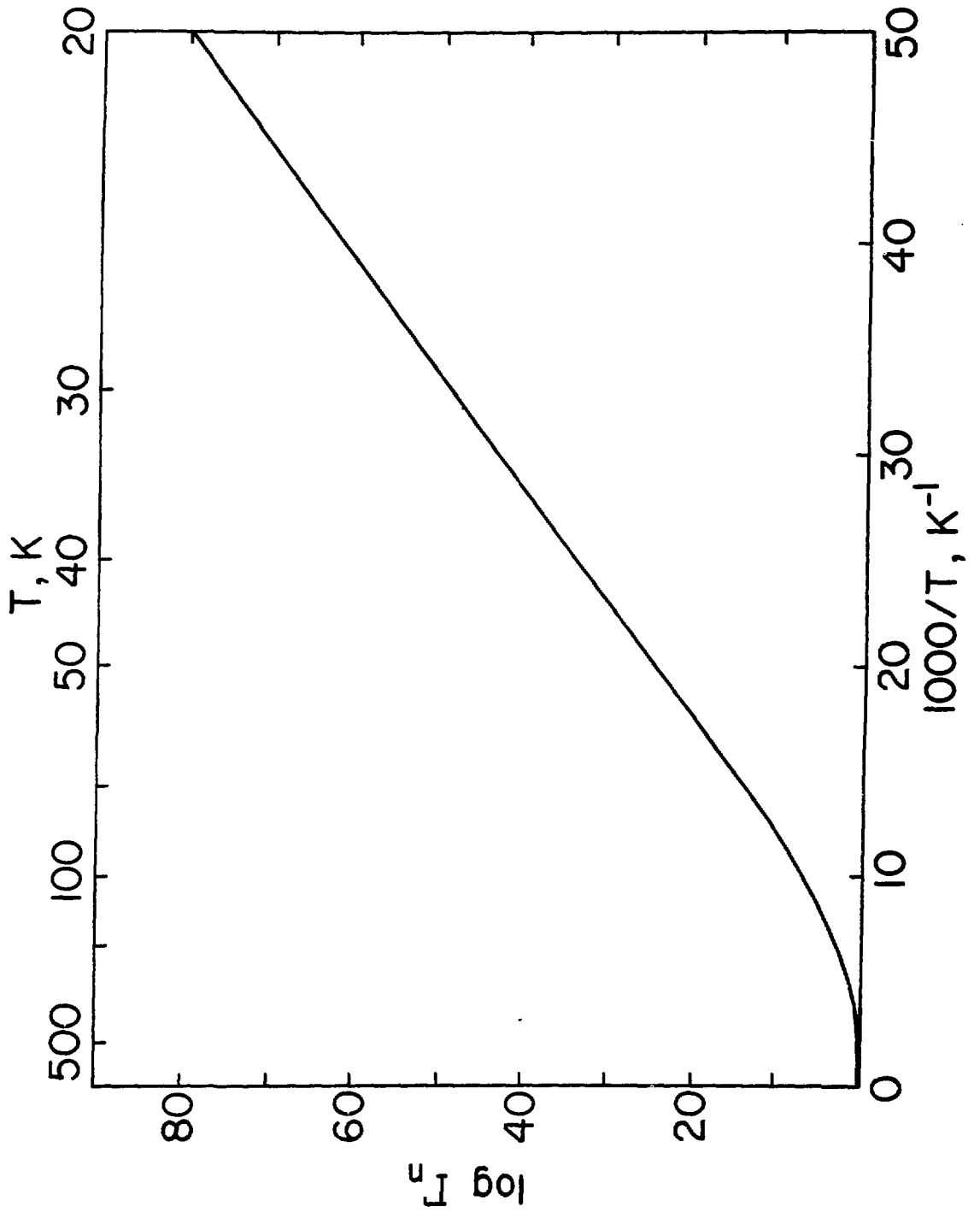


Figure 5

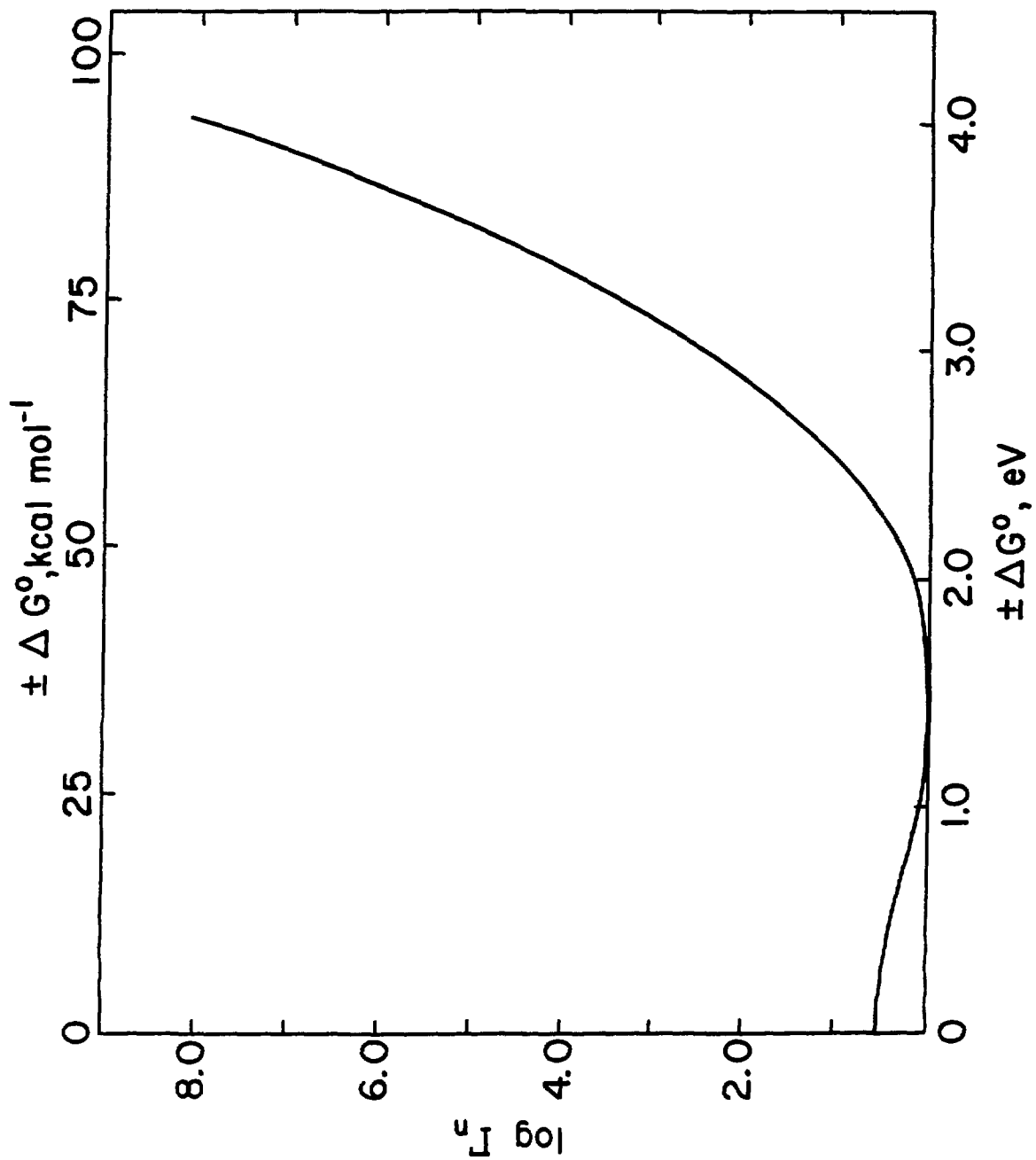


Figure 6